

PACS numbers: 42.62.Be; 87.15.–v; 87.64.K–; 87.85.Rs
DOI: 10.1070/QE2010v040n12ABEH014507

Laser-optical investigation of the effect of diamond nanoparticles on the structure and functional properties of proteins

E.V. Perevedentseva, F.Y. Su, T.H. Su, Y.C. Lin, C.L. Cheng, A.V. Karmenyan, A.V. Priezzhev, A.E. Lugovtsov

Abstract. **Adsorption of such blood plasma proteins as albumin and γ-globulin on diamond nanoparticles of size around 5 nm and around 100 nm is observed and studied using laser-optical methods. The adsorption of blood plasma proteins at physiological pH 7.4 is found weaker than that of enzyme protein lysozyme. The observed variations in the Fourier Transform Infrared (FTIR) spectra of proteins may be due to structural transformations of the adsorbed protein. Using the lysozyme as a test protein we show that the protein adsorption leading to observable changes in the FTIR spectrum (the band of Amide I) also induces a significant decrease in the protein functional activity. It is also found that the influence of ~5-nm diamond nanoparticles on the protein structure and functions is more significant than that of ~100-nm nanodiamonds.**

Keywords: *laser-optical methods, FTIR spectroscopy, nanodiamond, blood plasma proteins, adsorption.*

1. Introduction

The role of laser-optical methods in investigations of biological objects at various levels of organisation is constantly increasing [1, 2]. With the rapid development of nanotechnologies, these methods are widely used for solving the problems of nanobiophotonics, particularly, for studying the interaction of biologically important molecules with various nanoparticles, which can get into living (human) organism accidentally or intentionally. The sizes of nanoparticles are comparable with the characteristic sizes of biomolecules and/or cellular organelles; thus, the physical and chemical properties of such nanoparticles allow developing new methods and devices for applications in biological and medical investigations aiming, in particular, at the medical diagnostics and in future – at therapeutic treatment, as well as in biotechnologies.

E.V. Perevedentseva P.N. Lebedev Physics Institute, Russian Academy of Science, Leninsky prosp. 53, 119991 Moscow, Russia; present address: Physics Department, National Dong Hwa University, Hualien, Taiwan, e-mail: elena@mail.ndhu.edu.tw;
F.Y. Su, T.H. Su, Y.C. Lin, C.L. Cheng Physics Department, National Dong Hwa University, Hualien, Taiwan, e-mail: clcheng@mail.ndhu.edu.tw;
A.V. Karmenyan Institute of Biophotonics Engineering, National Yang Ming University, Taipei, Taiwan;
A.E. Lugovtsov, A.V. Priezzhev Department of Physics, International Laser Center, M.V. Lomonosov Moscow State University, Vorob'evy gory, 119991 Moscow, Russia, e-mail: avp2@mail.ru

Received 19 November 2010
Kvantovaya Elektronika **40** (12) 1089–1093 (2010)
Translated by E.V. Perevedentseva

Recently, nanodiamonds have started to attract the researchers' attention as nanoparticles promising for biomedical applications due to their optical, spectroscopic, electrochemical properties, structure and surface characteristics, size variability in a wide range, as well as due to low toxicity in comparison with other nanoparticles [3, 4]. First of all, a number of methods are being elaborated of a nanodiamond–biomolecules conjugation for obtaining new optical nanoprobes and nanosensors [3]. The nanodiamond has also a potential to be used for drug delivery [5, 6] and for such medical treatments [7] as hyperthermia or nanosurgery. On the other hand, in terms of rapid development of nanosciences and nanotechnologies, the problem of nanosafety becomes more and more important. Implementation of novel opportunities needs, at the same time, an extensive study of the impact of nanoparticles on the biological systems, when they directly or indirectly interact with each other. For example, studying the effect of nanoparticles on both the whole organism and individual organs and tissues needs the understanding of mechanisms of interaction of nanoparticles with blood, and hence with different blood components. However, the number of papers concerning the interaction of nanodiamond with biological objects at the tissue–organ–living organism level is still extremely low (see, e.g., [8, 9]).

This work aims at *in vitro* investigation of interaction of nanodiamonds measuring 5–10 nm and 100–130 nm with main blood plasma proteins: albumin (which is about 60% of all plasma proteins) and γ-globulin (immunoglobulin). The proteins adsorption on nanodiamonds and related structural transformations and changes in their functional state were analysed. The changes in the protein functionality, in the present case – enzymatic activity, were observed using antibacterial protein lysozyme. This protein is contained in biological fluids, well-studied, and widely used in investigations as a test protein [10].

The interaction of blood with ultrafine detonation nanodiamonds (including 5–10-nm nanodiamonds used in this work) was previously studied in [11, 12]. Insignificant harmful effects on white blood cells and on some biochemical characteristics of blood were observed [11], as well as some haemolysis of RBC, supposedly connected with adsorption of plasma macromolecules on the nanoparticles which changes the blood osmotic characteristics. However, Puzyr et al. [12] point out that the observed effects are not significant. Wasdo et al. [13] studied the interactions of some blood plasma proteins including albumin and γ-globulin with nanoparticles including nanodiamonds with the average size of 75 nm. Under the *in vitro* conditions, the affinity of both albumin and γ-globulin to nanoparticles was found low. However, due to a high content of albumin in the blood plasma, it can be adsorbed by nanoparticles in significant quantities.

The variations in the structure of proteins during their adsorption on different solid surfaces, including nanodiamonds, were repeatedly studied by various laser-optical methods. Structural transformations of the proteins are closely connected with changes in their functional state [14–16], which is observed in various processes, including adsorption and interaction with adsorbent, and when the proteins function normally [17]. The structural changes during adsorption are determined by the protein properties (structure, charge, etc.), as well as by properties and structure of the adsorbent surface [18] (e.g. hydrophobicity or hydrophilicity, electric charge, etc., including the curvature for nanostructured surfaces). Particularly, the effect of the adsorbent surface on the properties of adsorbed albumin was observed and studied previously by the methods of circular dichroism measurements [19], fluorescence and Fourier Transform Infrared spectroscopy [19, 20], etc. [21–25].

In our work, the adsorption of blood plasma proteins on nanodiamonds was analysed using UV–visible absorption measurements, and structural changes in the adsorbed proteins were analysed using the FTIR spectroscopy, basing on the sensitivity of the Amide I, II FTIR peaks to the changes in the protein secondary structure [17, 26].

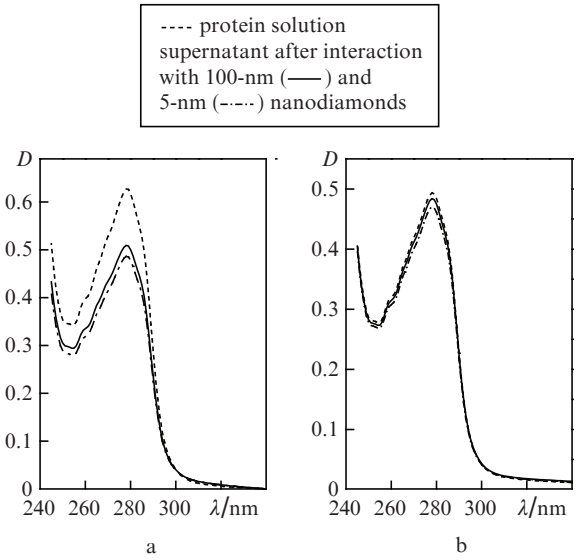

Figure 1. Absorption spectra of the albumin solution before the interaction with nanodiamond and after the adsorption on 100- and 5-nm nanodiamonds at pH around 5 (a) and 7.4 (b); *D* is the optical density.

2. Materials and methods

We used synthetic diamond powders with an average particle size of 5–10 nm (Microdiamant AG, Switzerland) and 100–130 nm (Kay Diamond, US). The particles were cleaned from surface nondiamond fractions, admixtures, and impurities using the standard method of treatment with strong acids ($H_2SO_4 : HNO_3 = 1:3$). This procedure also created carboxyl COOH-groups on the nanodiamond surface. Previously, it was shown that carboxylated nanodiamond has better biocompatibility [27], because surface molecular and ionic groups facilitate interaction of nanodiamond with biomolecules [28].

The proteins – human serum albumin, γ-globulin (both from Sigma, US), and lysozyme (Amresco, US) with the concentration of 40 mg mL^{-1} – were dissolved in bi-distilled water and mixed with water suspensions of nanodiamonds with the concentration of 4 mg mL^{-1} in the ratio 1:1. After 2 hours of thorough agitation, the mixture was centrifuged to separate the nanodiamonds with the adsorbed protein and residual protein solution. The sediment was washed with bi-distilled water to remove the nonadsorbed proteins.

The following laser-optical methods were used to investigate the prepared nanodiamond–protein complexes: the correspondence of the particle sizes to certificates was confirmed by measurements performed by the dynamic light scattering method using the DLS BI-200SM spectrometer (Brookhaven, US), equipped with a 523-nm diode-pumped solid-state laser. The ζ-potential of the particles was measured using the Zetasizer Nano ZS (Malvern Instruments, GB) with a 633-nm, 4-mW He–Ne laser.

The absorption spectra were measured with a dual-beam UV–visible JASCO V550 spectrophotometer (Japan). The absorption spectra of albumin solutions before and after adsorption on nanodiamonds are shown in Fig. 1. The absorption spectra of most proteins are characterised by the presence of the absorption band with a maximum near 280 nm. According to the Buger–Lambert–Beer law, the band intensity is proportional to the protein concentration in the solution. This allowed us to estimate the quantity of the protein adsorbed on the nanodiamond using the spectra of the initial protein solution and the supernatant – residual protein solution after adsorption.

We measured the FTIR spectra using the FTLA 2000 spectrometer (Bomem, Canada) equipped with a DTGS (Deuterated Triglycine Sulfate) detector. The samples were dropped on a Si substrate and dried in air; the measurements were also performed in air environment. Thus, we can assume that the protein state in the samples is analogous to that in the water solution or in prepared water suspensions, due to residual water, remaining bound with protein molecules. Note that the bound water is not observed in the measured FTIR spectra, probably, because there is only a limited amount of water in the samples. Moreover, the water absorption peaks are overlapped by Amide I and Amide II peaks (1655 and 1540 cm^{-1}) in the range of the bending mode of the water molecule vibration (1600–1630 cm^{-1}) and by Amides A, B bands (3100 and 3500 cm^{-1}) in the range of symmetric and asymmetric stretching modes (3200–3500 cm^{-1}).

The functional state of the protein adsorbed on nanodiamond was estimated for protein-enzyme lysozyme and was compared with the lysozyme activity in the water solution. The lysozyme concentrations in the control solutions were 0.03–0.12 mM and corresponded to lysozyme average concentrations in the suspensions of nanodiamonds with adsorbed lysozyme. To estimate the lysozyme enzymatic activity, we used the standard activity fluorescence test on the basis of the EnzChek Lysozyme E-22013 assay kit (Molecular Probes Inc., US). In this test, the effect of lysozyme on the cell wall of bacteria Micrococcus lysodeikticus is measured. The cell wall is labelled with fluorescein with the concentration at which the fluorescence in the intact cell wall is quenched. When lysozyme destroys the cell wall, the fluorescein fluorescence intensity increases and is proportional to the lysozyme concentration in the solution and its activity. Fluorescence was measured with the excitation wavelength of 485 nm and emission at 530 nm using a fluorescence microplate FluoroskanAscent reader (THERMO, US).

The pH of the suspensions and solutions, significantly determining the interaction between the investigated components, were controlled and measured with a SENTRON pH-meter (Titan, Taiwan).

3. Results and Discussion

Figure 1 shows the absorption spectra of albumin solutions before and after albumin adsorption on nanodiamonds of size 5 and 100 nm at pH in the range from 5 to 7.4. The difference in the intensities of the absorption bands before and after interaction of the protein with a nanodiamond suspension characterises the quantity of the albumin adsorbed on the diamond nanoparticles. One can see that the 5-nm nanodiamond adsorbs more protein than the 100-nm nanodiamond, because the total surface area of 5-nm nanodiamond particles is significantly larger than that for 100-nm particles in the suspension with the same weight concentration. Additionally, we should note that the structures of the used nanodiamonds (first of all, the structure of their surface) differ. The high content of diamond hybridization is characteristic of 100-nm nanodiamonds. Moreover, these nanoparticles are well enough dispersed in the suspension. On the surface of 5-nm nanodiamonds, carbon with a graphite structure or disordered carbon is predominant. In the suspension, aggregates and agglomerates of the nanoparticles are usually observed with a significantly irregular surface and inhomogeneous size [29]. Furthermore, nanodiamonds of size 5 and 100 nm differ in the ζ-potential which significantly determines the protein adsorption on nanodiamond.

The isoelectric point of albumin corresponds to pH 4.4–4.8 [30]. Thus, at pH close to the isoelectric point, when the albumin ζ-potential is close to neutral, a significant adsorption is observed. It can also be seen from the FTIR spectra (Fig. 2).

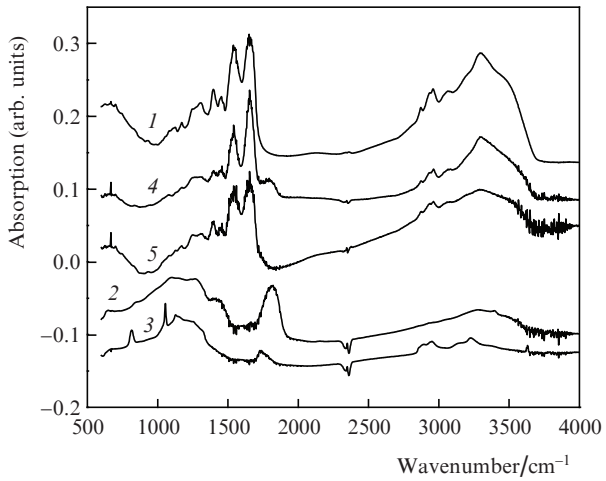

Figure 2. FTIR spectra of albumin (*1*), 100-nm (*2*) and 5-nm (*3*) nanodiamonds, and 100-nm (*4*) and 5-nm (*5*) nanodiamonds with adsorbed albumin; pH 5.

Figure 2 shows the spectra of 100- and 5-nm nanodiamonds, the albumin spectrum, and the spectra of the same nanodiamonds with adsorbed albumin. Note once more that the spectra of nanodiamonds with adsorbed albumin were measured after triple washing out of residual albumin in the solution. One can see that for the latter samples the protein spectrum significantly predominates over the nanodiamond spectrum. At pH 7.4 the protein signal is observed for the sample of 5-nm nanodiamond with adsorbed albumin [Fig. 3a, spectrum (*4*)] and is not observed for 100-nm nanodiamond after the protein adsorption (not shown). Adsorption of albumin on 5-nm nanodiamond occurs both at pH around 5 and 7.4. Note that in the pH range between 2 and 7.8, the values of the ζ-potential of 5-nm nanodiamond vary from +26 to +32 mV. The ζ-potential abruptly changes to a negative value at pH 8–9 and achieves –40 mV at pH 12.

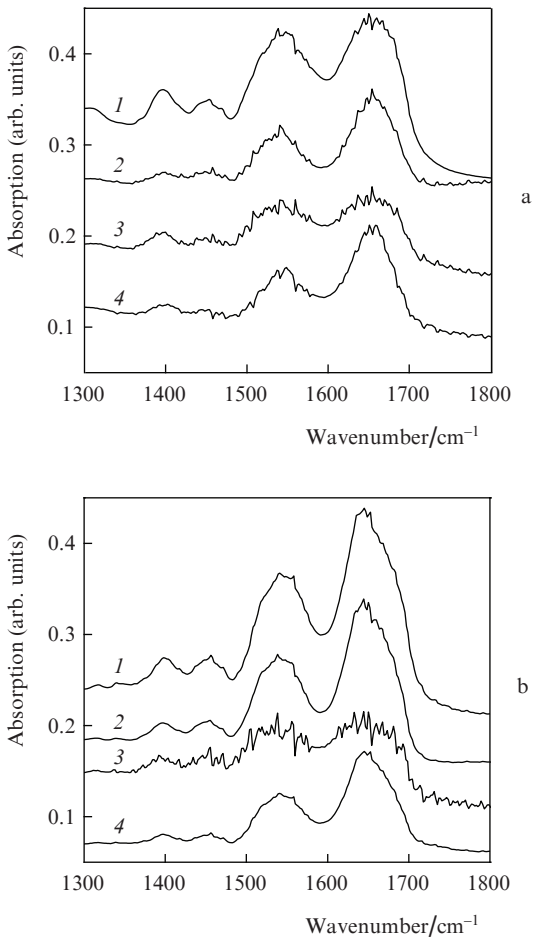

Figure 3. FTIR spectra of albumin (a) and γ-globulin (b) in the range of Amide I and II peaks: (*1*) protein; (*2*) protein adsorbed on 100-nm nanodiamond; (*3*, *4*) protein with 5-nm nanodiamond; pH 5.5 (*1*–*3*) and 7.4 (*4*).

We can assume that the major mechanism responsible for the albumin adsorption on nanodiamond is electrostatic attraction. This assumption is confirmed by the fact that the adsorption on 100-nm nanodiamond is negligible at physiologic pH (near 7.4), the particle's ζ-potential being negative (–40 to –50 mV) in a wide range of pH values.

Adsorption of γ-globulin on nanodiamonds was observed also at pH near 5–5.5 (Fig. 3b). Note that the isoelectric point of immunoglobulins takes the values in a wide pH range (6.7–9) [31]; thus, at physiologic pH values the immunoglobulins may be adsorbed on the nanodiamonds of size both 5 and 100 nm. The absorption spectra of the supernatant were analysed after centrifugation of the nanodiamond samples with protein adsorbed on the surface. The spectra after first as well as second and third washings of the samples from the nonadsorbed protein also confirm that the adsorption on 5-nm nanodiamond is more stable than on 100-nm nanodiamond – the adsorbed protein is not washed away.

Figure 2 presents the FTIR spectrum of albumin with absorption bands of Amide I (centred near 1655 cm^{-1}, arising mainly from stretching vibrations of C=O groups of the poly-

peptide chain), Amide II (centred near 1540 cm^{-1}, originating mainly from deformation bending NH groups of polypeptide backbone and side-chain vibrations), Amide III (a wide band in the range from 1200 to 1310 cm^{-1}, the vibrations of CN and NH groups), and the band near 1400 cm^{-1} originating from the symmetric vibration of the COO group, as well as the absorption bands of Amide A, B (3000–3300 cm^{-1}), which are characteristic of all proteins [17, 26, 32]. The variations in the peak intensity ratios and those in their components reveal the transformation of the protein secondary structure as a result of changes in relative contributions of such structural elements as α-helix, β-sheet, and the disordered fraction. The most intense component of the Amide I in the protein native state arises from stretching vibrations of C=O-groups comprised in the α-helix and the disordered part. The observed shift of the peak maximum reveals a relative increase in the contribution of C=O stretching of the β-sheet [26].

Figure 2 shows the FTIR spectra of nanodiamonds of size 100 nm (*2*) and 5 nm (*3*). The most characteristic and observable absorption bands in the FTIR spectrum of the carboxylated nanodiamond are related to C=O stretching (1700–1820 cm^{-1} depending on specific carbonyl-containing compound and its environment), hydroxyl-containing groups (~1640, 3400 cm^{-1}), asymmetric (2923 cm^{-1}) and symmetric (2855 cm^{-1}) vibrations of the C–H group, C–O–C and C–OH bonds (1100–1140 and 1360–1420 cm^{-1}) [29, 33]. Comparing spectra (*2*) and (*3*) with spectra (*4*) and (*5*) one can see that in the spectra of nanodiamonds with adsorbed albumin, the peaks corresponding to proteins, particularly, Amide I and Amide II significantly predominate over the OH and C=O peaks belonging to nanodiamond.

Figure 3 compares the FTIR spectra of dissolved albumin and γ-globulin in the Amide I, II range with the spectra of these proteins adsorbed on 100- and 5-nm nanodiamonds. One can see that changes in the Amide I shape and in the intensities ratio for Amide I, II, and III are observed for the nanodiamonds of both sizes at the albumin adsorption on them both at pH 5.5 [spectra (*2*,*3*)] and pH 7.4 [spectrum (*4*)]. For γ-globulin this effect was found less pronounced. The observed transformations of the spectra reveal a structural transformation of the protein molecules, but it is difficult to describe the changes in more detail.

The functional state of the proteins is determined to a significant degree by their structural state. Particularly, the structural transformation of albumin was observed at the performance of its transport function [34]. As for immunoglobulins, their structural–functional relations are extremely complicated. Even minor changes in the quaternary structure of the protein molecules can alter their function [35]. Thus, herein we want only to mention the importance of this investigation to estimate the possibility of the application of nanodiamonds *in vivo*.

To demonstrate the relation between the protein function and structural transformations caused by protein interaction with the nanodiamond surface during adsorption, we have used the enzyme lysozyme. Figure 4a shows the FTIR spectra in the Amide I, II range for lysozyme and lysozyme adsorbed on nanodiamond at pH around 6. Note that the isoelectric point of lysozyme corresponds to pH 11, stable and strong adsorption being observed in a wide range of pH (2–10) both on 100-nm nanodiamond (in this case the adsorption is determined by the electrostatic attraction between positive molecular groups in lysozyme and the negatively charged nanodiamond surface) and 5-nm nanodiamond, that has a positive

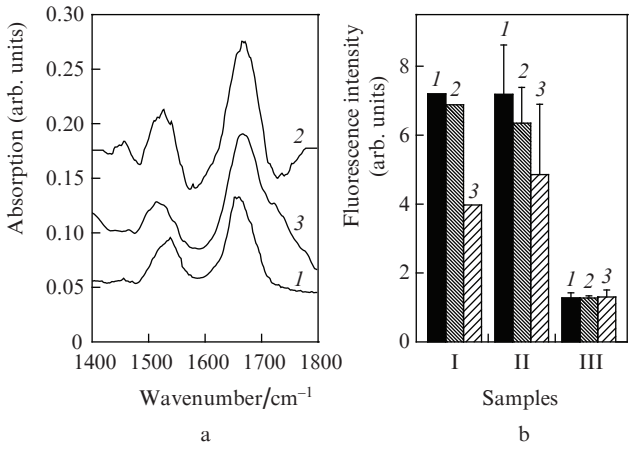

Figure 4. (a) FTIR spectra in the Amide I, II range [(*1*) lysozyme, (*2*) lysozyme adsorbed on 100-nm nanodiamond; (*3*) lysozyme adsorbed on 5-nm nanodiamond; pH 6]; (b) functional activity (proportional to the fluorescence intensity) of lysozyme in the water solution (sample I), lysozyme adsorbed on 100-nm nanodiamond (sample II), and lysozyme adsorbed on 5-nm nanodiamond (sample III); the lysozyme concentrations in the samples are as follows: (*1*) near 0.125 mM, (*2*) 0.03 mM, (*3*) 0.06 mM.

ζ-potential in the pH range from 2 to 8. The shift of the Amide I occurs from 1658 cm^{-1} for lysozyme to 1664 cm^{-1} for lysozyme adsorbed on 100-nm nanodiamond and to 1670 cm^{-1} for lysozyme adsorbed on 5-nm nanodiamond. In the latter case, the Amide I band also has an additional shoulder near 1720 cm^{-1}, which corresponds to the C=O stretching band of the nanodiamond carboxyl group. One can assume that the presence of this band reveals low ordering and inhomogeneity of the lysozyme layer on 5-nm nanodiamond. This is most likely due to such characteristic properties of 5-nm nanodiamond as the surface structure (e.g., the high content of the nondiamond fraction, many structural defects, positive ζ-potential), aggregation, significant surface curvature.

Figure 4b presents the results of investigation of the lysozyme functional state; the fluorescence intensities are compared for the samples, representing the lysozyme in the water solution and the lysozyme adsorbed on nanodiamonds. When using the EnzChek Lysozyme assay kit, the fluoresceine fluorescence intensity is proportional to the concentration of active lysozyme in the sample. The fluorescence intensities of the samples containing dissolved lysozyme and adsorbed lysozyme are practically similar and decrease proportionally to the decreasing concentration of lysozyme in the studied sample. The fluorescence intensity of the samples of the lysozyme adsorbed on 5-nm nanodiamonds is noticeably lower than fluorescence intensity of the control sample. It means that its functional antibacterial activity decreases sharply. Note that it is in agreement with previous investigations of cellular toxicity of nanodiamonds. It was shown that high concentrations of nanodiamonds of size 100 nm and above are not cytotoxic, while 5-nm nanodiamonds reveal some toxicity for the lung carcinoma A549 cells and for lung fibroblasts HFL1 [4, 27]. The difference in the impact of 100- and 5-nm nanodiamonds on the proteins are determined probably by a significant difference in the size, as well as by different structural and surface properties.

Since albumin is the main blood plasma protein, even the adsorption of its small part can affect the state of the blood plasma and, consequently, the state of blood in whole, par-

ticularly, the blood rheology. For γ-globulin, the importance of the present research is due to the fact that even minor transformations of the quaternary structure of the protein can impair its function and thereby the function of the organism immune system. Thus both nanodiamond and any other nanoparticles can be applied *in vivo* only after a thorough study of their interaction with all organism systems, including the blood plasma proteins.

4. Conclusions

Modern laser-optical methods allow observing the adsorption of such blood plasma proteins as albumin and γ-globulin on nanodiamonds of size 5 and 100 nm. It is shown that their adsorption is weaker than that of some other proteins (e.g., lysozyme), especially at the physiological pH value. However, the changes in FTIR spectra are observed, supposingly determined by structural transformations of the adsorbed protein. Using the lysozyme as a test protein, we have shown that the protein adsorption causing observable changes in the Amide I band of the FTIR spectrum also results in a significant decrease in the protein functional activity. It is revealed that 100-nm nanodiamond causes fewer variations in the protein structure and functional state in comparison with 5-nm nanodiamond.

According to the obtained results, we can conclude that safe applications of diamond nanoparticles *in vivo* as well as their wide use in blood investigations *in vitro* require meeting some special conditions. Thus, there arises a need in developing the methods for providing the necessary conditions, particularly, the ways to avoid spontaneous adsorption, and in the methods of the nanodiamond surface functionalisation. However, this requires further investigations.

Acknowledgements. This work was supported by the Russian Foundation for Basic Research (Grant No. 08-02-92002) and NSC of Taiwan (Grant No. NSC 97-2923-M-259-001-MY3).

References

1. Palumbo G., Pratesi R. *Lasers and Current Optical Techniques in Biology, Comprehensive Series in Photochemistry and Photobiology*. Ed. by D.P.Häder, G.Jori, (Cambridge, UK: Europ. Soc. for Photobiol., 2005) Vol. 4.
2. Tuchin V.V. *Lazery i volokonnaya optika v biomedetsinskikh issledovaniyakh* (Lasers and Fiber Optics in Biomedical Studies) (Moscow: Fizmatlit, 2010).
3. Krueger A. *Chem. Eur. J*., **14**, 1382 (2008).
4. Chao J.I., Perevedentseva E., Chung P.H., Liu K.K., Cheng C.Y., Chang C.C., Cheng C.L. *Biophys. J.*, **93**, 2199 (2007).
5. Chen M., Pierstorff E.D., Lam R., Li S.Y., Huang H., Osawa E., Ho D. *ASC Nano*, **7** (3), 2012 (2009).
6. Liu K.K., Zheng W.W., Wang C.C., Chiu Y.C., Cheng C.L., Lo Y.S., Chen C., Chao J.I. *Nanotechnol.*, **21**, 315106 (2010).
7. Chang C.C., Chen P.H., Chu H.L., Lee T.C., Chou C.C., Chao J.I., Su C.Y., Chen J.S., Tsai J.S., Tsai C.M., Ho Y.P., Sun K.W., Cheng C.L., Chen F.R. *Appl. Phys. Lett.*, **93**, 033905 (2008).
8. Yuan Y., Chen Y., Liu J.-H., Wang H., Liu Y. *Diamond Relat. Mater*., **18**, 95 (2009).
9. Mohan N., Chen C.S., Hsieh H.H., Wu Y.C., Chang H.C. *NanoLetters*, **10** (9), 3692 (2010).
10. Perevedentseva E., Cheng C.Y., Chung P.H., Tu J.S., Hsieh Y.H., Cheng C.L. *Nanotechnol.*, **18**, 315102 (2007).
11. Puzyr A.P., Neshumayev D.A., Tarskikh S.V., Makarskaya G.V., Dolmatov V.Yu., Bondar V.S. *Diamond Relat. Mater*., **13**, 2020 (2004).
12. Puzyr A.P., Baron A.V., Purtov K.V., Bortnikov E.V., Skobelev N.N., Mogilnaya O.A., Bondar V.S. *Diamond Relat. Mater.*, **16**, 2124 (2007).
13. Wasdo S.C., Barber D.S., Denslow N.D., Powers K.W., Palazuelos M., Stevens S.M. Jr., Moudgil B.M., Roberts S.M. *Int. J. Nanotechnol.*, **5** (1), 92 (2008).
14. Lynch I., Dawson K.A. *NanoToday*, **3** (1–2), 40 (2008).
15. Sethuraman A., Belfort G. *Biophys. J.*, **88**, 1322 (2005).
16. Zoungrana T., Findenegg G. H., Norde W. *J. Coll. Interface Sci.*, **190**, 437 (1997).
17. Barth A., Zscherp C. *Quart. Rev. Biophys*., **35**, 369 (2002).
18. Lück M., Paulke B.-R., Schröder W., Blunk T., Müller R.H. *J. Biomed. Mater. Res.*, **39**, 478 (1998).
19. Xiao Q., Huang S., Qi Z.D., He Z.K., Liu Y. *BBA*, **1784**, 1020 (2008).
20. Henry M., Dupont-Gillain C., Bertrand P. *Langmuir*, **19** (15), 6271 (2003).
21. Servagent-Noinville S., Revault M., Quiquampoix H., Baron M.-H. *J. Coll. Interface Sci.*, **221**, 273 (2000).
22. Sabatino P., Casella L., Granata A., Iafisco M., Lesci I. G., Monzani E., Roveri N. *J. Coll. Interface Sci.*, **314**, 389 (2007).
23. De Paoli Lacerda S.H., Park J.J., Meuse C., Pristinski D., Becker M.L., Karim A., Douglas J.F. *ASC Nano*, **4** (1), 365 (2010).
24. Ortega-Vinuesa J.L., Tengvall P., Lundstrom I. *Thin Solid Films*, **324**, 257 (1998).
25. Wangoo N., Suri C.R, Shekhawat G. *Appl. Phys. Lett*., **92**, 133104 (2008).
26. Tamm L.K., Tatulian S.A. *Quart. Rev. Biophys.*, **30** (4), 365 (1997).
27. Liu K.K., Cheng C.L., Chang C.C., Chao J.I. *Nanotechnol.*, **18**, 325102 (2007).
28. Chung P.H., Perevedentseva E., Tu J.S., Chang C.C., Cheng C.-L. *Diamond Relat. Mater*., **15**, 622 (2006).
29. Tu J.-S., Perevedentseva E., Chung P.-H., Cheng C.-L. *J. Chem. Phys*., **125**, 174713 (2006).
30. Oliva F.Y., Avalle L.B., Cámara O.R., De Pauli C.P. *J. Coll. Interface Sci.*, **261**, 299 (2003).
31. Li G., Stewart R., Conlan B., Gilbert A., Roerth P., Nair H. *Vox Sanguinis*, **83**, 332 (2002).
32. Jakobsen R.J., Wasacz F.M. *Appl. Spectr*., **44** (9), 1478 (1990).
33. Kulakova I. *Fiz. Tverd. Tela*, **46**, 621 (2004).
34. Reed R.G., Barrington C.M. *J. Biol. Chem.*, **264** (17), 9867 (1989).
35. Schroeder H.W. Jr., Cavacini L. *J. Allergy. Clin. Immunol*., **125** (2), S41 (2010).